

Journal of Materials Chemistry C

Accepted Manuscript



This article can be cited before page numbers have been issued, to do this please use: J. Yang, Z. Ren, B. Chen, M. Fang, Z. Zhao, B. Z. Tang, Q. Peng and Z. Li, *J. Mater. Chem. C*, 2017, DOI: 10.1039/C7TC03656F.



This is an Accepted Manuscript, which has been through the Royal Society of Chemistry peer review process and has been accepted for publication.

Accepted Manuscripts are published online shortly after acceptance, before technical editing, formatting and proof reading. Using this free service, authors can make their results available to the community, in citable form, before we publish the edited article. We will replace this Accepted Manuscript with the edited and formatted Advance Article as soon as it is available.

You can find more information about Accepted Manuscripts in the [author guidelines](#).

Please note that technical editing may introduce minor changes to the text and/or graphics, which may alter content. The journal's standard [Terms & Conditions](#) and the ethical guidelines, outlined in our [author and reviewer resource centre](#), still apply. In no event shall the Royal Society of Chemistry be held responsible for any errors or omissions in this Accepted Manuscript or any consequences arising from the use of any information it contains.



Journal Name

COMMUNICATION

Three polymorphs of one luminogen: How the molecular packing affects the RTP and AIE properties?

Received 00th January 20xx,
Accepted 00th January 20xx

DOI: 10.1039/x0xx00000x

www.rsc.org/

Polymorphism of organic molecules has received special attention, since the significantly different photophysical properties can provide important information to build a bridge between the micro- and macro-world. Here, we report three crystalline polymorphs of C2S-CN, which display much different properties of room temperature phosphorescence (RTP) and aggregation-induced emission (AIE). Due to the different molecular packing, the RTP lifetimes change from 266 ms to 41 ms, then to 32 ms, accompanying with the different photoluminescence quantum yields in crystal from 22.6% and 17.8% to 6.9%. Careful analyses on these crystal structures demonstrate that the properties are heavily related to the packing mode and molecular configuration, regardless of the same chemical structure, thus disclosing some important clues to understand the structure-packing-property relationship of RTP and AIE performance.

Organic π -conjugated molecules have attracted increasing attention for their potential applications in the fields of organic field-effect transistors (OFET), organic lasers, photovoltaic cells, stimuli-responses and so on.¹ Apart from the electronic nature of molecular structure, the molecular packing also shows large impact on the optoelectronic property, as functional π -conjugated molecules mainly exist in solid state for practical applications. Thanks to the enthusiasm of scientists, the investigation on how the molecular packing affecting related property has become a hot research topic.² Particularly, polymorphism of organic molecules has received special attention, since the different molecular packing often leads to the diverse properties, and the direct comparisons would be much beneficial to figure out the packing-property relationship,

^a Department of Chemistry, Hubei Key Lab on Organic and Polymeric Opto-Electronic Materials, Wuhan University, Wuhan 430072, China.

*Email: lizhen@whu.edu.cn or lichemlab@163.com

^b State Key Laboratory of Luminescent Materials and Devices, South China University of Technology, Guangzhou 510640, China.

^c Key Laboratory of Organic Solids, Beijing National Laboratory for Molecular Science (BNLMS), Institute of Chemistry Chinese Academy of Sciences, 100190 Beijing, China.

Electronic Supplementary Information (ESI) available: [Detail of synthesis, Figure S1-S19, Table S1-S4]. See DOI: 10.1039/x0xx00000x

Jie Yang,^a Zichun Ren,^a Bin Chen,^b Manman Fang,^a Zujin Zhao,^b Ben Zhong Tang,^b Qian Peng,^c and Zhen Li^{a,*}

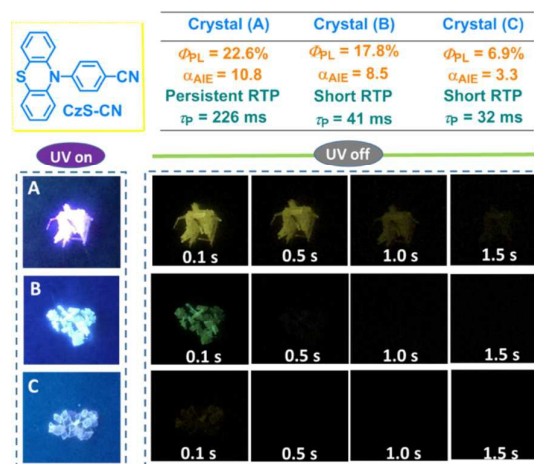


Figure 1 The molecular structure of C2S-CN and the related photoluminescence (PL) data about RTP and AIE properties (the α_{AIE} values are the ratio of PL quantum efficiencies in solid state and solution) for three polymorphs (upper); the photographs taken at different time, before and after turning-off the 365 nm UV-irradiation under ambient conditions (down).

then achieve the excellent optoelectronic performance.³ For example, Bao *et al.* successfully obtained previously unknown polymorphs of a small-molecule organic semiconductor with nearly order-of-magnitude improvement for its field-effect mobility (1.8 to $11 \text{ cm}^2 \text{ V}^{-1} \text{ s}^{-1}$);⁴ Wang *et al.* utilized a series of organic polymorphs for the different organic laser applicability;⁵ Seki *et al.* realized the mechano-responsive polymorphs with different emission colors (blue to yellow);⁶ and Hall *et al.* crystallized the polyaromatic hydrocarbon coronene in the presence of a magnetic field and obtained a β -herringbone structure instead of the ubiquitous γ -herringbone structure, accompanying with the extended absorptions from UV to near-IR.⁷

Recently, organic luminogens with room temperature phosphorescence (RTP) have attracted great attention for their full utilization of the excited state energy and long lifetime.⁸ However, most of the RTP systems contained noble metals,

COMMUNICATION

and the alternative metal-free phosphors were seldom reported, partially due to the lack of reliable guidance and unclear inherent mechanism.⁹ In this communication, we integrated phenothiazine and benzonitrile together to yield a new RTP luminogen of CzS-CN. Excitedly, through simply slow solvent evaporation in different initial solutions, three crystalline polymorphs were cultured including crystal (A), crystal (B) and crystal (C), which displayed different RTP lifetimes from 266 ms to 41 ms, then to 32 ms, accompanying with the different PL quantum yields from 22.6% and 17.8% to 6.9% (Figure 1 and Figure S1). Furthermore, CzS-CN was found to show typical characteristic of aggregation-induced emission (AIE, very weak emission in solution, however much enhanced one in aggregate and solid states). Once being ground, the PL emission peak could be tuned from 430 to 497 nm, indicating the highly contrast mechanochromism effect. Careful analyses of its crystal structures confirmed that the emissive properties are heavily related to the packing mode and molecular configuration. To the best of our knowledge, this is the first time to investigate the RTP and AIE effects with three polymorphs for the same luminogen. Herein, we present the synthesis, AIE, RTP and mechanochromism characterizations, crystal analyses and preliminary theoretical calculations of CzS-CN in detail, to understand the structure-packing-property relationship.

As shown in Scheme S1, CzS-CN could be conveniently synthesized through one step. Its UV-visible absorption spectrum was measured in THF solution. There were mainly two absorption peaks at 256 and 284 nm in deep violet region, indicating the limited conjugation (Table S1 and Figure S2). CzS-CN gave a very weak emission at about 529 nm in THF solution with a PL efficiency as low as 2.1%, mainly caused by the motions of phenothiazine, cyan groups and phenyl ring (Figure S3). After large amounts of water ($f_w > 90$), a poor solution, were added, the emission largely enhanced for the restricted intermolecular motions upon the formation of aggregates, demonstrating the AIE characteristic of CzS-CN.¹⁰

Three single crystals of CzS-CN were obtained through slow solvent evaporation, with their structural data summarized in Table S2. The powder X-ray diffraction (PXRD) measurement was carried out for the three polymorphs and powders. As shown in Figure 2A, these three crystals presented different PXRD peaks, indicating their different molecular packing. As for the as prepared powder, its PXRD peaks were similar to those of crystal (B), suggesting it mainly existed in the form of crystal (B). On the other hand, their PL spectra, including fluorescence and phosphorescence, and the corresponding lifetimes at room temperature as well as at 77K were also much different from each other (Figure S4-S8). Particularly, the RTP lifetimes for the three polymorphs could change from 266 ms to 41 ms, then to 32 ms (Figure 2B), accompanying with the different photoluminescence quantum yields from 22.6% and 17.8% to 6.9%.

Besides, CzS-CN showed much different emissive property in different powder states—as prepared, ground and fumed powders (Figure S9-S10). Particularly, its emissive peaks could change from 430 nm to 497 nm, just upon the simply

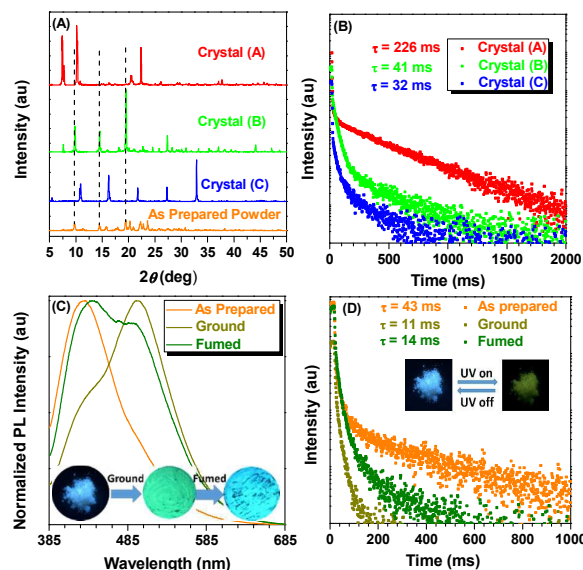


Figure 2 The changes of RTP lifetimes in different solid states. (A) PXRD patterns for CzS-CN in different crystal states and as prepared powder; (B) Time-resolved PL-decay curves for the room temperature phosphorescence in different crystal states; (C) PL spectra for the as prepared, ground and fumed CzS-CN powder (Insert: the photos for the as prepared, ground and fumed CzS-CN powder under 365 nm UV-irradiation); (D) Time-resolved PL-decay curves for their room temperature phosphorescence in different state (as prepared, ground and fumed) (Insert: the photos of as prepared CzS-CN powder taking at different times, before and after turning off the 365 nm UV-lamp).

mechanical stimulation (Figure 2C). The high contrast mechanochromism effect as large as 67 nm should be mainly originated from the transition from crystal to amorphous state as well as the structural co-planation.¹¹ In the meantime, its RTP effect also could be weakened by grinding, with RTP lifetimes shortening from 43 ms for the as-prepared powder to 11 ms in the ground state (Figure 2D). Thus, the different PL behaviors in different states could further prove the significant influence of molecular packing on the emissive property.

To explore the underlying mechanism of the emissive property of CzS-CN, the crystal analyses of these three polymorphs were further performed. First, the molecular configurations were taken into consideration for the possible influence on their emissive property, coupled with the preliminary theoretic calculations. As shown in Figure 3, the molecular configurations for CzS-CN in the three crystals were different from each other. In crystal (A), the molecule showed a highly twisted conformation with the torsion angel for phenothiazine moiety about 48° while about 117° between phenothiazine and benzonitrile groups. As for crystal (B), two minor different configurations, crystal (B1) and crystal (B2), were observed, which showed the similar torsion angels of 116° between phenothiazine and benzonitrile groups as crystal (A), but less twisted phenothiazine moieties with torsion angels of 42 – 43° . Differently, crystal (C) showed a more planar configuration in the long axis direction, with the torsion angels

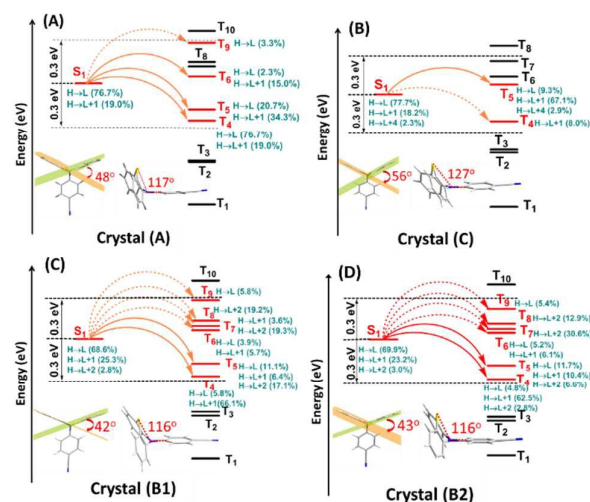


Figure 3 (A) The energy level diagram and molecular configuration for crystal (A); (B) The energy level diagram and molecular configuration for crystal (C); (C) The energy level diagram and molecular configuration for crystal (B1); (D) The energy level diagram and molecular configuration for crystal (B2).

between phenothiazine and benzonitrile groups about 127° , although it was 56° in the phenothiazine moiety. Thus, the different molecular configurations in crystals could surely make some influences on their different emissive properties.

In order to study the influence of the molecular configurations on their RTP effect, TD-DFT calculations on energy level and related excited state transition configurations for singlet and triplet states were carried out by b3lyp/6-31g* (Figure 3), based on the single crystals. The notations of H and L referred to the highest occupied molecular orbital (HOMO) and the lowest unoccupied molecular orbital (LUMO), while orange arrows referred to the possible ISC channels. The major ISC channels were mainly determined based on two elements— T_n gave a small energy gap (< 0.3 eV) with S_1 , and contained the same transition orbital compositions as S_1 state.^{8a} When the energy of T_n was similar or lower than that of S_1 , the latter element was considered to be more important. The determination of minor ISC channels was vice versa. For crystal (A), there were three major and one minor ISC channels, while those of crystal (C) were much less with only one major and one minor, owing to the big changes of the molecular configuration. Crystal (B1) and (B2) showed the same ISC transitions of two major and four minor ISC channels, for their similar molecular configurations. Thus, as demonstrated in the calculation results, more efficient ISC transitions of crystal (A) and (B) rather than those of crystal (C), could be in well accordance to their RTP properties, that is, crystal A and B gave much stronger RTP emissions than crystal (C) after turning off the UV-irradiation.

The theoretic analyses on $S_0 \rightarrow S_1$ transitions were carried out to explore the possible influence of molecular configurations on the different PL quantum yields.^[12] As shown in Figure S11 and Table S3, the electron coefficients in the HOMOs and

LUMOs all spread on the whole molecules, and the large overlap between

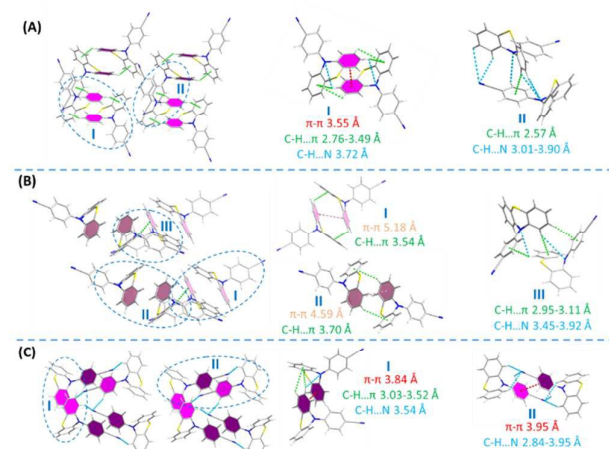


Figure 4 (A) Entire (left) and local (right) packing modes of the crystal (A) for Czs-CN; (B) Entire (left) and local (right) packing modes of the crystal (B) for Czs-CN; (C) Entire (left) and local (right) packing modes of the crystal (C) for Czs-CN. (The local packing pictures were selected from the parts in cycles of corresponding entire ones. In entire packing, the strong π - π interactions were labeled by pink color, weak π - π interactions were labeled by rose color and intermolecular hydrogen bonds less than 3.0 Å were linked, while in local packing, the intermolecular interactions were labelled and listed).

HOMOs and LUMOs could surely contribute much to their PL efficiencies. Among them, crystal (C) gave the highest oscillator strength (f) for the more planar configuration in the long axis direction, up to 0.21. However, crystal (A), (B1) and (B2) showed similar oscillator strength (f), from 0.12-0.13, for their minor different molecular configurations. Based on these calculations, crystal (C) should give the more efficient emission than others. But actually it was not, indicating that the molecular configuration could give some influence on the emissive property to some extent, but it was not the sole determining factor.

Generally, the main distinctions for polymorphs are the packing mode and molecular configuration. Thus, the molecular packing mode should be considered seriously. As shown in Figure 4, all of them showed different packing mode, accompanying with the diverse intermolecular interactions. In order to simplify the packing analyses and make a clear description of their distinctions, coupled units of two molecules with strong intermolecular interactions were selected and listed. In crystal (A), there were mainly two kinds of coupled units—coupled I and coupled II. In coupled I, two phenothiazine groups interacted with each other through π - π (3.55 Å), C-H... π (2.76-3.49 Å) and C-H...N (3.72 Å) bonds, while just hydrogen bonds of C-H... π (2.57 Å) and C-H...N (3.01-3.90 Å) were observed in coupled II. The strong intermolecular interactions would restrict the intermolecular motions effectively and lead to the reduced non-radiative transition, which could surely contribute much to the long RTP lifetime (266 ms), as well as its high PL quantum efficiency (22.6%).

However, the intermolecular interactions in crystal (B) were much weaker. Because of the existence of two different molecular configurations, three kinds of coupled units were observed. In coupled I and II (Figure 4B), two phenothiazine groups interacted with each other mainly through weak C-H... π bonds (3.54–3.70 Å), while multiple hydrogen bonds of C-H... π (2.95–3.11 Å) and C-H...N (3.45–3.92 Å) were found in coupled III. Thus, the weaker intermolecular interactions in crystal (B) would result in the short RTP lifetime (41 ms) and a relatively lower PL quantum efficiency (17.8%) in comparison with crystal (A). As for crystal (C) (Figure 4C), although multiple π - π (3.84 Å), C-H... π (3.03–3.52 Å) and C-H...N (3.54 Å) bonds in coupled I could restrict the non-radiative motions effectively, the formed H-type packing mode in coupled II, originated from the more planar configuration in the long axis direction, would result in the much lower PL efficiency (6.9%).¹² In crystal (A) and crystal (B), the more twisted configurations in the long axis made them tend to form X-type packing modes (couple II in crystal (A) and coupled III in crystal (B)), which could restrict the energy lose. Thus, their different packing modes, derived from the different molecular configurations, should be mainly responsible for their diverse AIE effects. As for the short RTP lifetime (32 ms) of crystal (C), it was the molecular configuration, rather than the packing mode, play the more significant role, for the less efficient ISC transition in that configuration.

To get a deep insight into how the packing mode affecting RTP process, the calculation on the energy levels were carried out on the coupled units picked from the single-crystal structures. Particularly, the energy gaps between S_1 and T_1 states were calculated for its significant role in the RTP process (Table S4, Figure S12).¹³ As shown in Figure S13, the energy gaps between S_1 and T_1 state in coupled units would decrease in comparison with those of isolated molecules, which could lead to the reduced energy lose in the process of internal conversion at excited triplet states, thus contribute much to the RTP effect. And, the coupled units with stronger intermolecular interactions tended to achieve smaller energy gaps between S_1 and T_1 states for the strong electron coupling effect. For the coupled I and II in crystal (A), they showed the smallest energy gaps, $\Delta(S_1-T_1)$, ranging from 0.64 to 0.74 eV, because of the strong intermolecular interactions. On the contrary, the coupled units in crystal (B), with relatively weak intermolecular interaction, gave the larger energy gaps, $\Delta(S_1-T_1)$, ranging from 0.81 to 0.91 eV. Thus, the smaller energy gaps between S_1 and T_1 states in crystal (A) could surely contribute much to its long RTP lifetimes of 266 ms rather than that (41 ms) of crystal (B). As for crystal (C), although the energy gaps in coupled units were moderate (from 0.80 to 0.86 eV), the inefficient ISC transitions, originating from the unique molecular configuration, have produced great limitations on its RTP effect. Thus different molecular packing, including molecular configuration and packing mode, should both be heavily related to the RTP effect.

As for the changed PL efficiencies in polymorphs, we tried to explore it through the transition dipoles in different packing modes. First, we calculated the directions of transition dipole

moments for isolated molecules in the three polymorphs, and found that all of them were parallel to the long axis (Figure S14). However, significant different transition dipole moments would occur in the different packing modes (Figure S15).¹⁴ In crystal (C), the coupled II presented a parallel stacking mode in the long axis, thus the lowest excited state corresponded to the destructive combination of the transition dipole moment for the individual molecule, which was optically forbidden and would result in the low PL efficiency (6.9%). As for crystal (A) and crystal (B), the more twisted configurations in the long axis made them tend to form X-type packing modes (couple II in crystal (A) with cross angle about 67° and coupled III in crystal (B) with cross angle about 62°), in which the energy splitting between the lowest two excited states of the coupled units would be much reduced, and a progressive transfer from the second excited state to the lowest excited state could occur. This level distribution promoted a finite transition dipole moment between the ground state and the lowest excited state, thus led to the much higher PL efficiencies—22.6% for crystal (A) and 17.8% for crystal (B).

As revealed by our experimental results, two main kinds of emissive properties, RTP and AIE ones, are heavily related to the molecular packing, including the molecular configuration and packing mode, in addition to the chemical structure. Actually, this viewpoint is applicable to other kinds of emissive property, such as PL emissive colors, mechanoluminescence (ML) and so on (Figure S16–S20). For example, Chi *et al.* identified that the different dipole moments, derived from the different molecular configurations in two polymorphs, determined whether there was the ML effect or not.¹⁵ Also, we proved that the packing mode with stronger intermolecular interactions in polymorphs played significant influence on the ML property in our previous work.¹⁶ As for the PL emission, Dong *et al.* got two kinds of crystals with blue and green emissions, and they ascribed it to their different distorted degrees in molecular configurations.¹⁷ Furthermore, Wang *et al.* could alter the PL emissions from yellow to red through simple heating, during which, the particular packing mode have changed from non-excimer to excimer.¹⁸ Besides these beautiful works, really scarce ones have concerned on polymorphs to explore the internal mechanisms of RTP and AIE effects. Particularly, the study on organic persistent RTP has been a new research area, and more thorough mechanisms are waiting for being revealed, and more efficient RTP luminogens are needed to be developed.

In summary, we have synthesized a new persistent RTP luminogen of CzS-CN. Furthermore, it was found to show interesting AIE and highly contrast mechanochromism effects. Particularly, three kinds of crystalline polymorphs for CzS-CN were cultured, in which the RTP lifetimes changed from 266 ms to 41 ms, then to 32 ms, accompanying with the different photoluminescence quantum yields from 22.6% and 17.8% to 6.9%. A careful analyses on these crystal structures, coupled with theoretical calculations, demonstrated that the emissive properties are heavily related to the molecular packing, including molecular configuration and packing mode, even for the same compound. Thus, the information gained from this

work could help us to make a deep understanding of structure-packing-property relationship and provide some guidance in the design of other RTP and AIE luminogens. In addition, molecular packing should also be considered seriously for other photophysical process in condensed state. Only with it, a deep and thorough understanding could be obtained.

Conflicts of interest

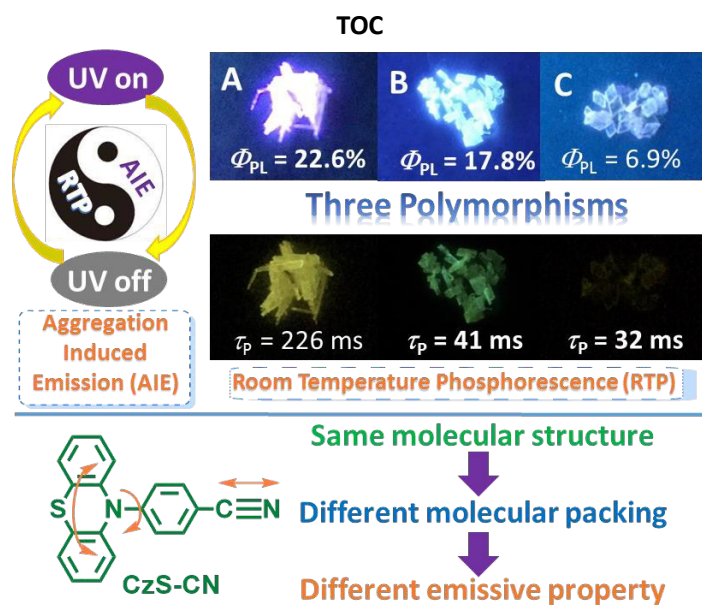
There are no conflicts to declare.

ACKNOWLEDGMENT

We are grateful to the National Science Foundation of China (no. 21325416, 51573140) and National Fundamental Key Research Program (2013CB834701) for financial support.

References

- [1] (a) J. B. Birks, *Photophysics of Aromatic Molecules*, Wiley, London, **1970**; (b) B. Valeur, *Molecular Fluorescence: Principle and Applications*, Wiley, Weinheim, **2005**.
- [2] (a) B. Fraboni, A. Fraleoni-Morgera, Y. Geerts, A. Morpurgo, V. Podzorov, *Adv. Funct. Mater.*, **2016**, **26**, 2229-2232; (b) J. Zhang, W. Xu, P. Sheng, G. Zhao, D. Zhu, *Acc. Chem. Res.*, **2017**, DOI: 10.1021/acs.accounts.7b00124; (c) A. Mannix, X. Zhou, B. Kiraly, J. Wood, D. Alducin, B. Myers, X. Liu, B. Fisher, U. Santiago, J. Guest, M. Yacaman, A. Ponce, A. Oganov, M. Hersam, N. Guisinger, *Science*, **2015**, **350**, 1513-1516.
- [3] (a) M. Baroncini, S. Agostino, G. Bergamini, P. Ceroni, A. Comotti, P. Sozzani, I. Bassanetti, F. Grepioni, T. Hernandez, S. Silvi, M. Venturi, A. Credi, *Nat. Chem.*, **2015**, **7**, 634-640; (b) X. Meng, B. Gui, D. Yuan, M. Zeller, C. Wang, *Sci. Adv.*, **2016**, **2**, e1600480; (c) A. Pulido, L. Chen, T. Kaczorowski, D. Holden, M. Little, S. Chong, B. Slater, D. McMahon, B. Bonillo, C. Stackhouse, A. Stephenson, C. Kane, R. Clowes, T. Hasell, A. Cooper, G. Day, *Nature*, **2017**, **543**, 657-664; (d) S. Mondal, G. Mugesh, *Angew. Chem.*, **2015**, **127**, 10983-10987; (e) M. Jin, T. Seki, H. Ito, *J. Am. Chem. Soc.*, **2017**, **139**, 7452-7455.
- [4] (a) G. Giri, E. Verploegen, S. Mannsfeld, S. Atahan-Evrenk, D. Kim, S. Lee, H. Becerril, A. Aspuru-Guzik, M. Toney, Z. Bao, *Nature*, **2011**, **480**, 504-508; (b) Y. Diao, B. Tee, G. Giri, J. Xu, D. Kim, H. Becerril, R. Stoltenberg, T. Lee, G. Xue, S. Mannsfeld, Z. Bao, *Nat. Mater.*, **2013**, **12**, 665-671; (c) J. Anthony, *Nat. Mater.*, **2014**, **13**, 773-775.
- [5] K. Wang, H. Zhang, S. Chen, G. Yang, J. Zhang, W. Tian, Z. Su, Y. Wang, *Adv. Mater.*, **2014**, **26**, 6168-6173.
- [6] H. Ito, M. Muromoto, S. Kurenuma, S. Ishizaka, N. Kitamura, H. Sato, T. Seki, *Nat. Commun.*, **2013**, **4**, 2009.
- [7] J. Potticary, L. Terry, C. Bell, A. Papanikolopoulos, P. Christianen, H. Engelkamp, A. Collins, C. Fontanesi, G. Kociok-Kohn, S. Crampin, E. Como, Simon. Hall, *Nat. Commun.*, **2016**, **7**, 11555.
- [8] (a) Z. An, C. Zheng, Y. Tao, R. Chen, H. Shi, T. Chen, Z. Wang, H. Li, R. Deng, X. Liu, W. Huang, *Nat. Mater.*, **2015**, **14**, 685-690; (b) Zhao, W. Z. He, J. Lam, Q. Peng, H. Ma, Z. Shuai, G. Bai, J. Hao, B. Tang, *Chem.*, **2016**, **1**, 592-602; (c) Y. Gong, G. Chen, Q. Peng, W. Yuan, Y. Xie, S. Li, Y. Zhang, B. Tang, *Adv. Mater.*, **2015**, **27**, 6195-6201; (d) Z. Yang, Z. Mao, X. Zhang, D. Ou, Y. Mu, Y. Zhang, C. Zhao, S. Liu, Z. Chi, J. Xu, Y. Wu, P. Lu, A. Lien, M. Bryce, *Angew. Chem.*, **2016**, **128**, 2221-2225; (e) Y. Shoji, Y. Ikabata, Q. Wang, D. Nemoto, A. Sakamoto, N. Tanaka, J. Seino, H. Nakai, T. Fukushima, *J. Am. Chem. Soc.*, **2017**, **139**, 2728-2733; (f) J. Yang, Z. Ren, Z. Xie, Y. Liu, C. Wang, Y. Xie, Q. Peng, B. Xu, W. Tian, F. Zhang, Z. Chi, Q. Li, Z. Li, *Angew. Chem.*, **2017**, **129**, 898-902.
- [9] (a) S. Xu, R. Chen, C. Zheng, W. Huang, *Adv. Mater.*, **2016**, **28**, 9920-9940; (b) S. Hirata, *Adv. Optical Mater.*, **2017**, 1700116; (c) M. Baroncini, G. Bergamini, P. Ceroni, *Chem. Commun.*, **2017**, **53**, 2081-2093; (d) S. Mukherjee, P. Thilagar, *Chem. Commun.*, **2015**, **51**, 10988-11003.
- [10] J. Mei, N. Leung, R. Kwok, J. Lam, B. Tang, *Chem. Rev.*, **2015**, **115**, 11718-11940.
- [11] C. Wang, Z. Li, *Mater. Chem. Front.*, **2017**, DOI: 10.1039/C7QM00201G.
- [12] Q. Qi, J. Qian, X. Tan, J. Zhang, L. Wang, B. Xu, B. Zou, W. Tian, *Adv. Funct. Mater.*, **2015**, **25**, 4005-4010.
- [13] Y. Gong, L. Zhao, Q. Peng, D. Fan, W. Yuan, Y. Zhan, B. Tang, *Chem. Sci.*, **2015**, **6**, 4438-4444.
- [14] Z. Xie, B. Yang, F. Li, G. Cheng, L. Liu, G. Yang, H. Xu, L. Ye, M. Hanif, S. Liu, D. Ma, Y. Ma, *J. Am. Chem. Soc.*, **2005**, **127**, 14152-14153.
- [15] B. Xu, J. He, Y. Mu, Q. Zhu, S. Wu, Y. Wang, Y. Zhang, C. Jin, C. Lo, Z. Chi, A. Lien, S. Liu, J. Xu, *Chem. Sci.*, **2015**, **6**, 3236-3241.
- [16] C. Wang, B. Xu, M. Li, Z. Chi, Y. Xie, Q. Li, Z. Li, *Mater. Horiz.*, **2016**, **3**, 220-225.
- [17] Z. He, L. Zhang, J. Mei, T. Zhang, J. Lam, Z. Shuai, Y. Dong, B. Tang, *Chem. Mater.*, **2015**, **27**, 6601-6607.
- [18] M. Yuan, D. Wang, P. Xue, W. Wang, J. Wang, Q. Tu, Z. Liu, Y. Liu, Y. Zhang, J. Wang, *Chem. Mater.*, **2014**, **26**, 2467-2477.



Three crystalline polymorphs of CzS-CN, which display much different properties of room temperature phosphorescence (RTP) and aggregation-induced emission (AIE). Careful analyses on these crystal structures demonstrate that the properties are heavily related to the packing mode and molecular configuration, regardless of the same chemical structure.

View Article Online
DOI: 10.1039/C7TC03656F